JOURNAL OF Materials CHEMISTRY

A comparison of direct synthesis and vapour phase alumination of MCM-41

Afshin Ghanbari-Siahkali, Andreas Philippou, Arthur Garforth, Colin S. Cundy, Mike W. Anderson and John Dwyer*

UMIST Centre for Microporous Materials, Department of Chemistry, UMIST, PO Box 88, Sackville Street, Manchester, UK M60 1QD. E-mail: John.Dwyer@umist.ac.uk

Received 24th May 2000, Accepted 12th September 2000
First published as an Advance Article on the web 28th November 2000

Mesoporous AlMCM-41 materials were prepared by both direct synthesis and the reaction of siliceous MCM-41 with aluminium chloride vapour. The products were characterised using XRD, N_2 sorption, EDAX and both MAS NMR and FTIR spectroscopy, and acid catalytic activity was evaluated using the conversion of 1,3,5-triisopropylbenzene (1,3,5-TIPB) as a test reaction. Acid site concentrations (Brønsted and Lewis) were estimated from sorption of pyridine, using FTIR. The concentrations of acid sites were correlated with the fraction of aluminium in the solids and comparisons were made with results published previously for similar mesoporous materials. Both the compositions of the gels used in the synthesis of Al-mesoporous materials and the procedures used to introduce aluminium into mesoporous silica strongly influenced the above correlation. In all cases, the ratio of total acid site concentration to aluminium concentration was less than unity. Consideration of the present catalytic results for conversion of 1,3,5-TIPB along with results published previously for conversion of cumene, demonstrates that acid catalytic activity is better correlated with Brønsted rather than with Lewis site concentration.

Introduction

The catalytic activity of zeolites has, in several instances, been shown to be directly proportional to the framework aluminium content.[1,2] It is well documented that the properties of zeolites can be modified by dealumination, steaming or/and acid leaching procedures or by the insertion of aluminium into siliceous microporous materials.[3–6] Recently, there has been considerable interest in applying similar techniques to tailor the acidity and hence the catalytic activity of mesoporous MCM-41 materials,[7–22] which have potential as catalysts for the conversion of species too bulky to react within zeolite pores.

Procedures are well described[23] for the direct synthesis of mesoporous MCM-41 materials containing aluminium incorporated into the siliceous frameworks and, by varying the source of aluminium and silicon and the type of template, it has been possible to achieve Si/Al values as low as 2.[8,11,12] In all cases the materials prepared by direct synthesis are reported to have acid sites of only medium strength.[24–27] The aluminium sites in mesoporous AlMCM-41 do not, in all cases, appear to be involved in acid catalysed reactions, presumably because some of them exist within the pore walls (thickness 10–20 Å) and are inaccessible to reactants or because they are not appropriately coordinated to generate acidity. Consequently, there is interest in improving the accessibility of Al sites by introducing aluminium into the siliceous mesoporous framework by post-synthesis treatments. Several such procedures are described[18–22,28] and in all cases the approach has involved the reaction of a siliceous mesoporous phase with a solution containing aluminium or by wet impregnation of the siliceous phase with an aluminium salt.

In the present paper we explore the possibility of introducing aluminium into siliceous MCM-41 frameworks by solid/vapour reactions, a procedure which has been used to introduce acid sites (bridged hydroxyls) into zeolites,[3–5] and to graft chlorided alumina sites onto silica surfaces.[29] A series of AlMCM-41 catalysts having varying aluminium content, where the aluminium is incorporated directly during synthesis (denoted hereafter, D), is compared with catalysts prepared by post-synthesis, using the reaction of aluminium chloride vapour with siliceous MCM-41 (denoted hereafter, P). The materials are characterised by powder XRD, chemical analysis, N_2 sorption and spectroscopic techniques, including MAS NMR (^{27}Al, ^{29}Si, ^{1}H) and FTIR. For both series the concentrations of Brønsted and Lewis sites are estimated from the FTIR spectra of sorbed pyridine and are compared with results reported[21,22,28] for direct synthesis of AlMCM-41 using different sources of silicon and aluminium, and also with Al-MCM-41 materials prepared by reaction of siliceous mesoporous materials with solutions of aluminium species. Acid catalytic activity is assessed using the conversion of 1,3,5-triisopropylbenzene (1,3,5-TIPB) as a test reaction and the results are discussed in relation to studies reported previously for the conversion of cumene over acidic mesoporous catalysts. The role of Brønsted and Lewis sites is examined.

Experimental

Synthesis

Aluminosilicate AlMCM-41. Following a modified synthesis procedure,[23] AlMCM-41 materials were synthesised as follows: 0.78 g of sodium aluminate (32.7 wt% Al_2O_3, 28.5 wt% Na_2O, 39.0 wt% H_2O, BDH) was dissolved in 42.0 g of C_{16}TMACl solution (hexadecyltrimethylammonium chloride, 25.0 wt%, Aldrich). The resulting solution was combined with 11.0 g of TMAOH·$5H_2O$ (tetramethylammonium hydroxide pentahydrate, 97.0 wt%, Janssen Chemica), 1.6 g of NH_4OH (35.0 wt% solution, Fisons, UK), 12.0 g of fumed silica (Cabosil M-5, BDH) and 23.0 g of distilled water. The mixture was stirred for 12 hours to produce a gel having composition:

$$Al_2O_3 : 80SiO_2 : 13.1C_{16}TMACl : 11.8(TMA)_2O : 6.4NH_4OH : 1352H_2O$$

The reaction mixture was loaded into autoclaves and heated

statically at 110 °C for 72 hours. The solid product was recovered by filtration, washed repeatedly with deionised water and dried in air at room temperature. The template within the pore structure was carefully removed by calcination at 540 °C for 1 hour in a nitrogen flow, followed by 6 hours in a flow of air at the same temperature. The N_2/air flows and heating rates were 100 ml min^{-1} and 1 °C min^{-1} respectively.

Purely siliceous SiMCM-41. Pure-silica SiMCM-41 material was also synthesised as described above with the omission of the sodium aluminate.

Post-synthesis AlMCM-41. The reactor[30] was a quartz glass tube (1 cm i.d. × 45 cm length) with a ball joint at each end. A four-way valve permitted a purge gas flow in either direction through the tube and out *via* the vent. A tube furnace heated two thirds of the length of the reaction vessel. The reactor could be adjusted and moved inside the furnace. In a typical experiment, purely siliceous SiMCM-41 (0.51 g) was loaded into the centre of the reactor on one side and anhydrous Al halide (0.24 g) was loaded on the other side. A quartz wool plug separated the two sections. The temperature was raised to 361 °C (5 °C min^{-1}) and held for 1 hour under a dry N_2 flow (50 ml min^{-1}) entering *via* the halide end of the reactor. The system was subjected to a change in flow direction every 10 minutes in order to recover the condensed Al halide at the downstream end of the reactor tube by moving this cold end to the furnace-heating zone. The treated sample was calcined at 500 °C (5 °C min^{-1}) under N_2 followed by air (50 ml min^{-1}) for 1 hour. Both (D)/AlMCM-41 and (P)/AlMCM-41 were ion-exchanged, after calcination, using NH_4NO_3 (1 M) solution at room temperature for 12 hours. The solid to solution ratio was 1 g : 100 ml. The solids were recovered by centrifuging and washing with distilled water and dried at 100 °C for 4 hours.

Characterisation

X-Ray powder diffraction data were obtained using a Scintag XDS 2000 diffractometer with θ–θ geometry, Cu-Kα radiation and an energy dispersive X-ray detector. Diffraction patterns were recorded using continuous scanning at a rate of 1.0 degrees per minute. Elemental analysis of the samples was obtained using a Philips SEM 525-20 kV fitted with an EDAX 9100/60 energy dispersive spectrometer. Textural properties were determined from nitrogen adsorption isotherms at 77 K using a manual gravimetric technique with a CAHN D-200 recording microbalance (CAHN Instruments, USA) described as a force-to-current converter. Prior to the adsorption experiments, the samples were out-gassed at 300 °C under vacuum (10^{-5} Torr) overnight. The acidic nature of MCM-41 materials was investigated by FTIR spectroscopy in the region of OH vibrations and of pyridine complexes. FTIR spectra of chemisorbed pyridine were measured *in situ* using a Nicolet Magna 550 FTIR spectrometer. The sample, activated at 350 °C under vacuum (10^{-5} Torr) for several hours, was exposed to pyridine at 150 °C followed by evacuation at 150 °C and 10^{-5} Torr for half an hour to remove physisorbed pyridine. Then the spectrum was recorded at ambient temperature. ^{29}Si and ^{27}Al magic-angle spinning MAS NMR spectra were recorded at room temperature on a Bruker MSL 400 spectrometer using a Bruker 7 mm probe with a spinning rate of *ca.* 5 kHz and a 4 mm probe with a spinning rate of *ca.* 9 kHz respectively. ^{29}Si and ^{27}Al MAS NMR spectra and chemical shifts were referenced to external tetramethylsilane and aqueous aluminium nitrate respectively. The ^{1}H MAS NMR spectra of dehydrated samples were recorded at room temperature using a Bruker 4 mm probe with a spinning rate of *ca.* 9 kHz and chemical shifts are referenced to external tetramethylsilane.

Catalysis

The activity of the catalysts in the H-form was tested using 1,3,5-TIPB (97.0% pure) in the gas phase at both 450 °C and 370 °C and at atmospheric pressure, in a fixed-bed flow reactor (Pyrex) system. Results were compared with those for a commercial amorphous silica–alumina catalyst (Crosfield Catalyst, UK). The catalyst (0.5 g) was placed in the reactor bed, and gently tapped to ensure good radial distribution and quartz wool was inserted over the catalyst bed. The reactor was placed in a three-zone furnace, with the catalyst bed positioned in the middle zone. A syringe pump delivered a uniform flow of 12 ml h^{-1} during the reaction (60 minutes, time-on-stream). Dry nitrogen was used as a carrier and the carrier/reactant molar ratio was 2.0 throughout. Complete evaporation of the feed was ensured prior to entry to the catalyst bed, and during the course of the catalytic run, by measuring temperatures at several points in the heating zone above the bed (up to 12 cm) and simultaneously at the surface of the bed. Prior to catalytic reactions, all catalysts (250–425 μm, pellet size) were activated *in situ* at 540 °C for four hours in a stream of dry nitrogen (30 ml min^{-1}). Gas products were analysed by GC-FID (Varian 3400) using a PLOT Al_2O_3 KCl, 50 m × 0.32 in diameter, fused silica capillary column (Chrompack). Liquid products were analysed by GC (Varian 3400) fitted with a BP 21, 25 m × 0.25 in diameter, fused silica polar column. Individual products were identified by GC-MS using commercially available reference mixtures. Good mass balances were obtained and the main products were diisopropylbenzenes, cumene, benzene and propene. Fresh catalyst was used in each run to reduce the effect of deactivation.

Results and discussion

Fig. 1 shows the X-ray powder diffraction patterns of purely siliceous SiMCM-41 after calcination, (P)/Na-AlMCM-41 and in the H-form. The positions of the SiMCM-41 peaks fit the positions of the *hkl* reflections for a hexagonal lattice ($a_0 = 2d_{100}/\sqrt{3}$) as described by Beck *et al.*,[23] and the quality of the X-ray pattern for (P)/AlMCM-41 is comparable with that of the parent (SiMCM-41) materials [Fig. 1(c)]. The intensity of the (100) peak after treatment with $AlCl_3$ becomes slightly broader but remains almost unchanged, and the (110), (200) and (210) reflections become less well defined. The position of the (100) peak shifts slightly towards higher *d*-spacing resulting in an increase in the unit cell constant of treated samples (Table 1). Borade and Clearfield[11] reported a shift of the most intense peak towards higher *d*-spacing with an increase in the alumina content of AlMCM-41. These results are consistent with an increase in pore size of the aluminated MCM-41 materials, associated with insertion of some Al into the structural framework.[7,11] Fig. 2 shows the X-ray powder diffraction patterns of a (D)/AlMCM-41 sample before and after calcination and after generation of the H-form. These patterns are comparable with those reported in the literature for AlMCM-41.[23] As can be seen from Figs. 1 and 2, the X-ray patterns of (D)/AlMCM-41 are less well defined compared to (P)/AlMCM-41 at different stages of preparation. This evidence suggests that (D)/AlMCM-41 samples may be less ordered than the (P)/AlMCM-41 or, alternatively, possess considerable amounts of local defects within the mesopore structure. The local disorder in the (D)/AlMCM-41, which has been reported previously,[28] is mainly associated with the incorporation of Al species within the framework of mesoporous materials.

Nitrogen adsorption on all the MCM-41 samples (Fig. 3) shows typical type-IV isotherms.[31] The isotherm for (P)/AlMCM-41 is comparable with that of the parent material, which suggests that the mesoporosity of the treated sample is largely preserved during post-synthesis alumination. Textural

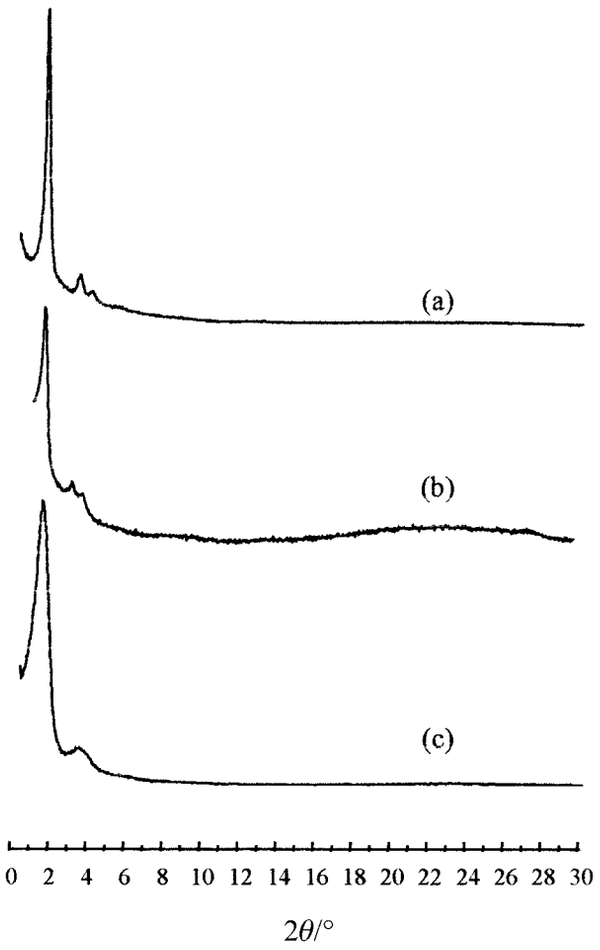

Fig. 1 X-Ray diffraction patterns of (a) calcined SiMCM-41, (b) calcined (P)/Na-AlMCM-41 and (c) (P)/H-AlMCM-41.

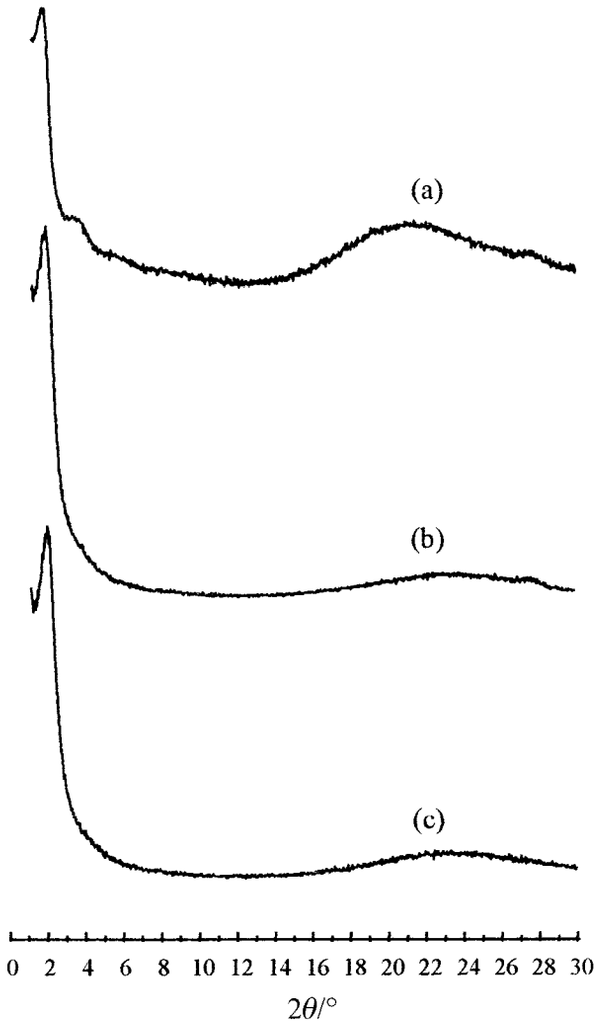

Fig. 2 X-Ray diffraction patterns of direct synthesis (a) (D)/AlMCM-41, (b) calcined (D)/Na-AlMCM-41 and (c) (D)/H-AlMCM-41.

and physical properties of the samples studied in the present work are given in Table 1.

Fig. 4 shows FTIR spectra of (P)/AlMCM-41, (D)/AlMCM-41 and silica–alumina in the region of 1400–1600 cm^{-1}. Pyridine was used as a probe molecule in studying the acidic properties of samples prepared in this work. Concentrations of pyridine on Brønsted and Lewis sites were estimated using the extinction coefficients described by Emeis,[32] assuming the interaction of one pyridine molecule with one Brønsted acid site. In a previous study of acid zeolites[33] we have shown that, when Brønsted acid sites are proximate, a single pyridine molecule can form a pyridinium ion which is strongly hydrogen bonded to neighbouring Brønsted sites. In such cases the assumption that one pyridine molecule interacts with one Brønsted site to provide one pyridinium ion is not true. Since we do not know the distribution of Brønsted sites in AlMCM-41 materials there must be some uncertainty about the 1 : 1 assumption and, consequently, about reported extinction coefficients. However, for lower levels of aluminium (higher Si/Al) we might reasonably expect the 1 : 1 assumption to become valid and the use of common extinction coefficients provides a basis for comparison of the data.

Table 1 Textural properties of the samples studied by N_2 adsorption

Sample	Unit cell[a]/Å	BET/$m^2\ g^{-1}$	Pore volume /$cm^3\ g^{-1}$	Mean pore size/Å
(D)/AlMCM-41	53.9	618	0.54	35
SiMCM-41	54.4	443	0.35	29.5
(P)/AlMCM-41[a]	54.4	403	0.33	30.0
Silica–alumina	—	292	0.54	—

[a]The unit cell has been calculated from the interplanar spacing using the formula $a_0 = 2d_{100}/\sqrt{3}$.

All samples containing aluminium exhibit bands at 1545 cm^{-1} and 1455 cm^{-1}, which are assigned to Brønsted and Lewis acid sites respectively. The signal at 1495 cm^{-1} has been assigned previously to a combination band associated with both Brønsted and Lewis sites.[34] For purely siliceous SiMCM-41 no signal was observed in the region from 1400 cm^{-1} to 1600 cm^{-1} on adsorption of pyridine. Fig. 5 shows FTIR spectra of the parent material (SiMCM-41), (P)/AlMCM-41 and (D)/AlMCM-41 in the OH region with a band centred at 3745 cm^{-1}, assigned to isolated silanol groups, and a broad band ranging from 3700 cm^{-1} to 3500 cm^{-1} assigned to hydrogen bonded hydroxyl groups. As expected, the adsorption of pyridine did not result in a change in the spectrum of SiMCM-41. For both (P)/AlMCM-41 and (D)/AlMCM-41 samples there is a loss in the intensity of the band at 3745 cm^{-1} due to interaction with adsorbed pyridine (Fig. 5).

Fig. 6 illustrates the ^{29}Si MAS NMR spectra of Al/SiMCM-41 samples prepared by both post and direct synthesis methods. The ^{29}Si MAS NMR spectrum of calcined SiMCM-41, the parent material used in the post-synthesis method, is shown in Fig. 6(a). This spectrum displays the typical pattern of SiMCM-41 and is the composite of three rather broad signals at −108, −100 and −91 ppm assigned to Q_4, Q_3 and Q_2 units respectively.[35] Post-synthesis aluminium insertion into the SiMCM-41 structure followed by ammonium exchange and calcination to produce (P)/H-AlMCM-41 leads to a broadening of all resonances. As shown in Fig. 6(b), the spectrum of (P)/H-AlMCM-41 exhibits one broad signal centred at *ca.* –107 ppm.

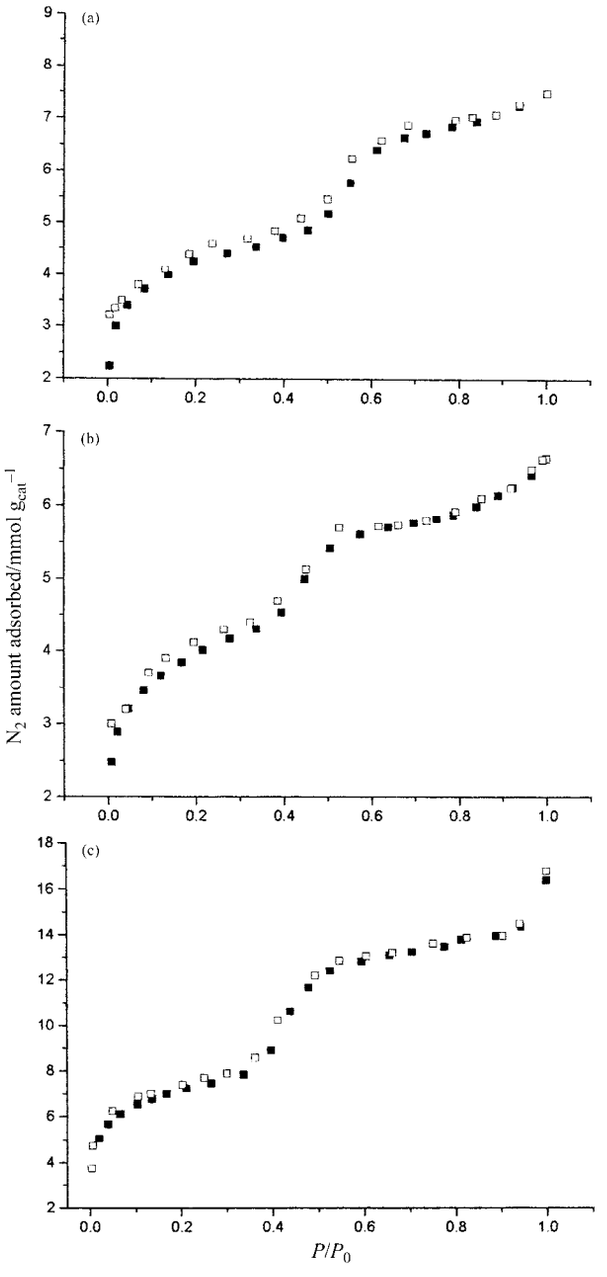

Fig. 3 N_2 adsorption isotherms of (a) calcined SiMCM-41, (b) (P)/AlMCM-41 and (c) (D)/AlMCM-41. The filled and empty symbols denote adsorption and desorption respectively.

The ^{29}Si MAS NMR spectra of AlMCM-41 samples prepared by direct synthesis methods are shown in Fig. 6(c) to (e). The spectrum of calcined (D)/Na-AlMCM-41, shown in Fig. 6(c), displays three signals at *ca.* −110, −100 and −90 ppm which are assigned to Q_4, Q_3 and Q_2 units, respectively, as above. Furthermore, the presence of aluminium in the SiMCM-41 structure must form a chemical environment [Si (3Si, 1Al)], which, presumably, contributes to the resonance at −100 ppm.[8] Ammonium exchange to produce (D)/NH_4-AlMCM-41 leads to a considerable increase of the signals at *ca.* −100 and −90 ppm [Fig. 6(d)], which may result from generation of Q_3 and Q_2 units. As discussed subsequently, calcination of (D)/NH_4-AlMCM-41 to form (D)/H-AlMCM-41 leads to a considerable broadening of all signals. The spectrum of (D)/H-AlMCM-41, shown in Fig. 6(e), displays one broad line at *ca.* –107 ppm. At this stage it is worth noting that, due to the amorphous nature of these solids, ^{29}Si MAS NMR provides no clear evidence as to aluminium incorporation into the SiMCM-41 structure.

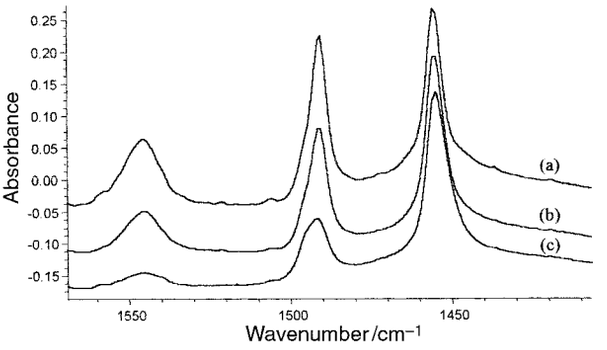

Fig. 4 FTIR spectral region showing the Brønsted (1545 cm^{-1}) and Lewis (1455 cm^{-1}) bands region for (a) (P)/H-AlMCM-41, (b) (D)/H-AlMCM-41 and (c) H-form silica–alumina.

Unlike ^{29}Si MAS NMR, the application of ^{27}Al MAS NMR yields more direct information as to the fate of aluminium in these studies. Fig. 7(a) shows the ^{27}Al MAS NMR spectrum of (P)/NH_4-AlMCM-41 where two lines at *ca.* 54 and 0 ppm are attributed to framework tetrahedral and extraframework octahedral aluminium respectively. Calcination of (P)/NH_4-AlMCM-41 to produce (P)/H-AlMCM-41 has a profound effect on the ^{27}Al MAS NMR spectrum as shown in Fig. 7(b). The spectrum of (P)/H-AlMCM-4 exhibits three resonances at 54, 30 and 0 ppm. The lines at 54 and 0 ppm are assigned as above whereas the signal at 30 ppm is attributed to either framework or extraframework pentacoordinated aluminium. Seemingly, the calcination process has dislodged or partially dislodged a considerable amount of framework aluminium to produce extraframework sites or higher coordination framework sites.

Fig. 7(c) illustrates the ^{27}Al MAS NMR spectrum of calcined (D)/Na-AlMCM-41 where a line at 54 ppm is assigned to framework tetrahedral aluminium and a rather broad and featureless signal, covering from *ca.* −200 to 100 ppm, is assigned to very distorted aluminium in both framework and extraframework sites. Calcination to remove the organic template results in considerable removal of framework

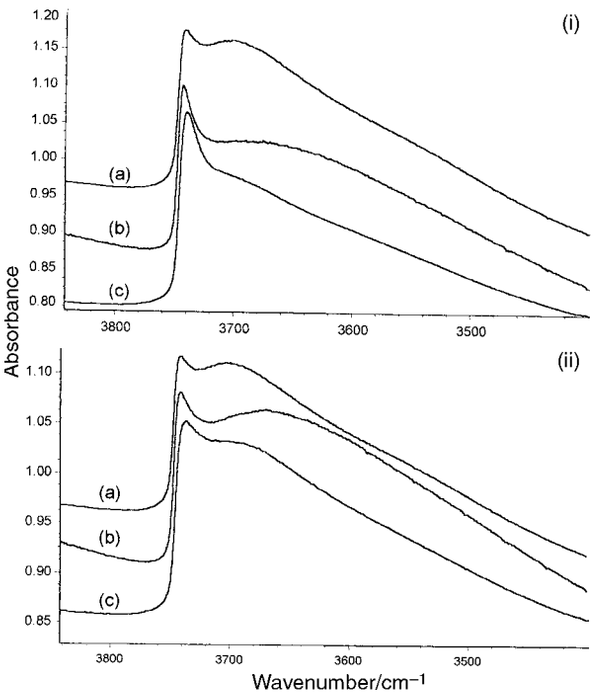

Fig. 5 FTIR spectra of the hydroxyl region, (i) before and (ii) after pyridine adsorption on (a) SiMCM-41, (b) (P)/H-AlMCM-41 and (c) (D)/H-AlMCM-41.

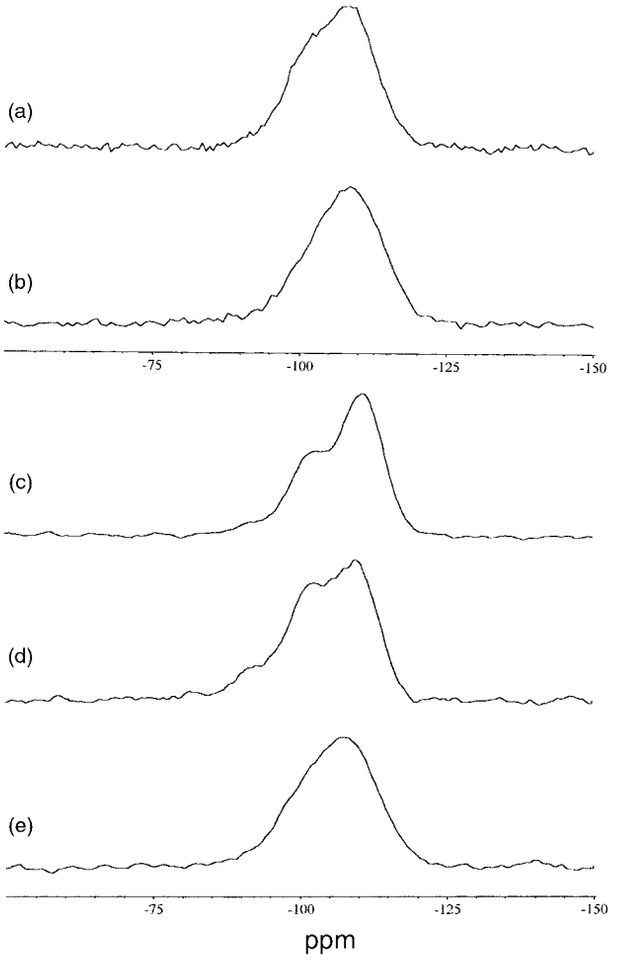

Fig. 6 ^{29}Si MAS NMR spectra of (a) calcined SiMCM-41, (b) (P)/H-AlMCM-41, (c) calcined (D)/Na-AlMCM-41, (d) (D)/NH4-AlMCM-41 and (e) (D)/H-AlMCM-41.

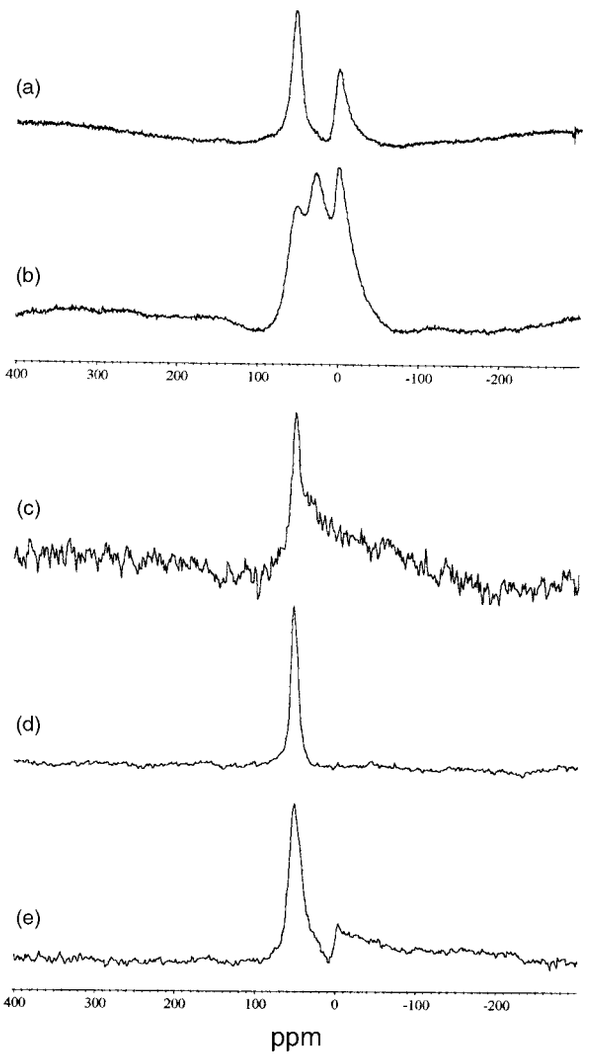

Fig. 7 ^{27}Al MAS NMR spectra of (a) (P)/NH_4-AlMCM-41, (b) (P)/H-AlMCM-41, (c) calcined (D)/Na-AlMCM-41, (d) (D)/NH_4-AlMCM-41 and (e) (D)/H-AlMCM-41.

aluminium to extraframework sites while it must also have distorted framework sites.

Ammonium exchange of calcined (D)/Na-AlMCM-41 has a rather extraordinary effect on the ^{27}Al MAS NMR spectrum of this material. Fig. 7(d) illustrates the ^{27}Al MAS NMR spectrum of (D)/NH_4-AlMCM-41 where only one strong signal at *ca.* 54 ppm is detected and assigned to framework tetrahedral aluminium. Bearing in mind that these spectra were recorded under almost identical conditions (*i.e.* number of scans and amount of sample) one may pursue a comparison between the spectra in Figs. 7(c) and (d). Ostensibly, the intensity of the signal at 54 ppm in Fig. 7(d) has increased markedly at the expense of the broad resonance which may suggest that the liquid phase ammonium exchange has reinserted extraframework aluminium into the framework to produce tetrahedral sites. However, this assumption is not supported on the grounds of further experimental findings discussed subsequently. Chemical analysis of the liquid recovered after the ammonium exchange clearly indicates the presence of aluminium, which in turn verifies the removal of extraframework aluminium upon ion-exchange. Furthermore, the degree of hydration of these samples has a profound effect on the signal intensity in these spectra and should, therefore, be considered carefully. The ^{27}Al MAS NMR spectrum of the re-hydrated (D)/Na-AlMCM-41 (not shown) exhibits the same features as that of Fig. 7(c) with an additional narrow line at 0 ppm, assigned to hydrated and symmetric extraframework octahedral aluminium, while the signal at 54 ppm also gains intensity. All things considered, the strong signal at 54 ppm in Fig. 7(d) results mainly from hydration of framework tetrahedral sites while the absence of any upfield signals is due to removal of extraframework aluminium upon ammonium exchange.

As expected, calcination of (D)/NH_4-AlMCM-41 to produce (D)/H-AlMCM-41 leads to a loss of framework aluminium and an increase in extraframework aluminium sites. Fig. 7(e) depicts the ^{27}Al MAS NMR spectrum of (D)/H-AlMCM-41 displaying a line at 54 ppm, assigned as above, and a very broad signal covering from *ca.* −250 to 0 ppm attributed to distorted extraframework octahedral aluminium. Both the line shape and width of this signal indicate a strong second order quadrupolar interaction resulting from a distorted aluminium environment.

Fig. 8 illustrates the ^{1}H MAS NMR spectra of (a) (P)/H-AlMCM-41 and (b) (D)/H-AlMCM-41. These spectra exhibit a very similar pattern with a strong resonance at *ca.* 1.8 ppm assigned to non-acidic terminal silanol protons and a rather weak and broad signal centered at *ca.* 3.0 ppm which may be attributed to Q_3 hydrogen-bonded and Q_2 hydroxyl protons. The weak signal at *ca.* 7 ppm in the ^{1}H MAS NMR spectrum of (D)/H-AlMCM-41 (Fig. 8(b)) is assigned to residual NH_4^+ cations. The generation of Brønsted acidity may contribute to the resonance at 3.0 ppm as the FTIR experiments clearly indicate the presence of Brønsted acidity in these systems. The difficulty in detecting Brønsted acidity in these ^{1}H MAS NMR experiments must relate to strong homonuclear dipolar

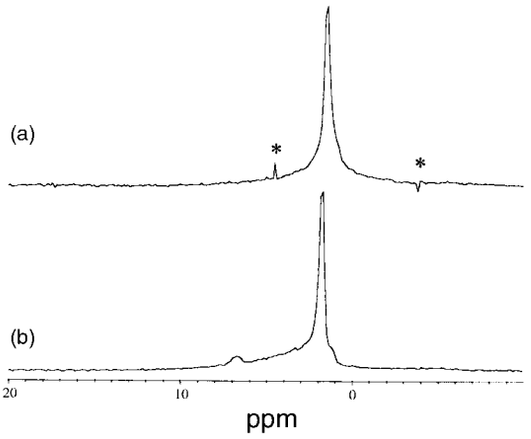

Fig. 8 ^{1}H MAS NMR spectra of (a) (P)/H-AlMCM-41 and (b) (D)/H-AlMCM-41; asterisks denote artefacts.

interactions and/or hydrogen bonding, both of which lead to a considerable line broadening.

In summary, the MAS NMR findings demonstrate that AlMCM-41 materials generated by either direct or post-synthesis methods contain aluminium in both framework and extraframework positions. Although it is difficult to quantify the ^{27}Al MAS NMR results, because of second order quadrupolar effects, it is evident that a significant amount of aluminium moves to extraframework sites during the calcination of the ammonium form to produce the hydrogen form of the catalysts. This loss of framework aluminium is associated with a reduction in long range order, which is also observed by other techniques including XRD (Fig. 1). It is generally accepted that extraframework aluminium is associated with Lewis acidity. In the post-synthesised materials extraframework aluminium is observed with both octahedral and pentacoordination, whereas only six coordinated aluminium was observed in directly synthesised AlMCM-41. Consequently, ^{27}Al MAS NMR results suggest that increased concentrations of Lewis acid sites might be expected in the post-synthesised catalysts and this expectation is confirmed by the FTIR study.

Reaction of $AlCl_3$ vapour with hydroxylated silicate

The reaction between aluminium chloride vapour and zeolites (Y and ZSM-5) and with silica has been reported.[3–5] At the temperatures typically used to vaporise aluminium chloride the vapour phase consists mainly of the dimer (Al_2Cl_6), but for simplicity, the reaction between a mole of $AlCl_3$ and up to three surface hydroxyls may be written:

$$n(\equiv SiOH) + AlCl_3 \rightarrow (\equiv SiO)_n AlCl_{3-n} + nHCl \qquad (1)$$

For reaction with silica gel[9] the surface species formed depend on the preparation of the chlorided silicas, depending in particular on the temperature of activation of the silica gel and the temperature of reaction between silica gel and aluminium chloride. In the present study any chloride, associated with Al_2Cl_6 grafted onto the silica, should be largely or completely removed by hydrolysis during the ion-exchange procedures. Consequently, we should expect surface species of type $(\equiv SiO)_n Al(OH)_{3-n}$ with $n=1$ to 3. Reaction of Al_2Cl_6 with a nest of four hydroxyls may be represented as:

$$4(\equiv SiOH) + 2AlCl_3 \rightarrow [(\equiv SiO)_4 Al]AlCl_2 + 4HCl \qquad (2)$$

In this case, ion-exchange with aqueous ammonia followed by activation at elevated temperature should generate bridged Brønsted sites, [≡Si(OH)Al≡]. Information on the coordination of aluminium to oxygen, or to chloride, can be provided by ^{27}Al MAS NMR spectra. Very extensive studies on hydrothermally synthesised zeolites and related materials, have revealed up to at least three types of aluminium coordinated to oxygen as mentioned earlier in connection with Fig. 7.

The ^{27}Al MAS NMR spectra, discussed previously (Fig. 7), provide no evidence for aluminium linked to chlorine ligands, which give signals with increased chemical shifts compared to oxygen ligands.[9] Such species are not expected after the extensive hydrolysis used in the present work and, in support of this, elemental analysis showed only traces of chloride on the solid.

Following catalytic runs a ^{27}Al MAS NMR signal around 33 ppm is clearly evident for the (P)/H-AlMCM-41 materials and it may be assigned to aluminium pentacoordinated to oxygen. Aluminium species having higher coordination to oxygen (five or six) are associated with the development of strong Lewis acid sites, and can, by appropriate interaction, also result in the development of Brønsted sites having enhanced acidity.[36] The catalytic activity of purely siliceous MCM-41 treated with $AlCl_3$ was compared with that of (D)/AlMCM-41 and also with a commercial sample of amorphous silica–alumina having a Si/Al ratio of 4 (Table 2) using the conversion of 1,3,5-TIPB as a test reaction. The catalytic results show clearly that the (P)/H-AlMCM-41 is more active than the other catalysts both at 450 °C and 370 °C. Purely siliceous MCM-41 did not show any activity.

The generation of acid sites in mesoporous aluminosilicates

(a) By direct synthesis. This feature has been very widely studied in recent years[12,16,18–20,22,25,28] and considerable differences in both direct synthesis and post-synthesis procedures are reported. In the case of direct synthesis the major differences may be illustrated by the components used to form the synthesis gels (Table 3). This table is not comprehensive but includes syntheses where aluminium is reported to be extensively incorporated in tetrahedral sites. The purpose of incorporating aluminium into these materials is to produce acid sites and several papers provide results on the measurement of acidity and of acid catalysis. Fig. 9 provides a comparison of the present results with previously published reports where measurements of both Brønsted and Lewis acid site concentrations, determined by pyridine sorption, are given. All data are corrected to concentrations based on the IMEC values of Emeis.[32] These are preferred to the IMEC values of Hughes and White,[37] since, for example, the IMEC for the pyridinium ion determined by Emeis lies close to recently reported values.[38]

From Fig. 9 it seems clear that, at lower levels of aluminium incorporation, the different synthesis procedures result in materials giving a similar pattern for the dependence of Brønsted acid concentration on the weight fraction of aluminium [Al/(Al+Si)] in the catalysts [Fig. 9(a-i)] and Table 3. At low levels of aluminium there is evidence that synthesis gels using alkoxides of aluminium and silicon give higher concentrations of Brønsted sites than gels prepared from conventional and cheaper sources of Si and Al. The role of template (amine *versus* quaternary) does not appear, on the basis of the results in Fig. 9(a-i) and Table 3, to make a major difference when alkoxides are used as sources for Si and Al. As the level of aluminium in the solids increases, the increase in Brønsted acid concentration levels off in all cases but the results of Chen *et al.*[21] show significantly higher concentrations of Brønsted sites than synthesis procedures based on amine templates[13] or based on conventional sources of silica and alumina[23] [Fig. 9(a-i)]. In all cases, even at low levels of aluminium, the concentration ratio of Brønsted to Lewis sites is less than one and in general the ratio Lewis/Brønsted is not, greatly, dependent on the level of aluminium. The dependence of total acid site concentration, represented here by the sum of Brønsted and Lewis acid sites, on aluminium fraction [Fig. 9(a-ii)] follows a pattern similar to that for Brønsted sites [Fig. 9(a-

Table 2 Summary of catalytic conversion of 1,3,5,-TIPB over catalysts prepared in this work

Catalyst	Temperature/°C	Conversion[a]/mol%	Mass balance/wt%	Coke/wt%	k/Al[b]
(P)/AlMCM-41	450	94.0	96.0	4.3	50.18
(17)	370	37.9	96.7	6.1	8.57
(D)/AlMCM-41	450	73.1	97.2	8.0	40.94
(30)	370	22.2	97.4	10.2	7.81
Silica–alumina	450	34.1	97.0	17.3	2.51
(4)	370	14.2	98.2	21.5	0.90

Reaction parameters: pressure = 1 atm, WHSV = 12 h^{-1}, W/F = 5 (W = weight, F = flow rate, WHSV = weight hourly space velocity). The number in parentheses represents the bulk Si/Al ratio in wt% as measured by EDAX. [a]Conversion here given after one hour on stream. [b]Relative pseudo first order rate constant, k/Al fraction, calculated from $\ln(1/1-x)$ where x is the conversion.

Table 3 Typical reagents used in recently reported syntheses of mesoporous aluminosilicates

Materials	Silica source	Alumina source	Template	Reference
MCM-41	Fused silica (Cabosil)	$Al_2(SO_4)_3$	CTAM(OH)	8, 13
MCM-41	TEOS	$Al(OPr^i)_3$	CTAM(OH)	21
SAB-15	TEOS	$Al(OPr^i)_3$	Triblock copolymers	37
MCM-41	TEOS	$NaAlO_2$	CTMACl	17
MMS	TEOS	$Al(OPr^i)_3$	DDCA	28

TEOS: Tetraethylorthosilicate, CTAM(OH)/Cl: cetyltrimethylammonium hydroxide/chloride, triblock copolymers: poly(ethylene oxide)–poly(propylene oxide)–poly(ethylene oxide), DDCA: dodecylamine.

i)]. This is expected because of the (approximate) constancy of the site ratio Lewis/Brønsted. At increased levels of aluminium, higher concentrations of total acidity are achieved in the synthesis reported by Chen *et al.*[21] (Table 3). However, at lower levels of aluminium the results for total acidity in the present study are closer to those (Table 3) reported by Mokaya *et al.*[13] than is the case for Brønsted site concentration [Fig. 9(a-i)]. This is, presumably, because of the dealumination which occurs during the calcination and ion-exchange procedures which are necessary to produce the hydrogen forms of AlMCM-41 prepared using inorganic sources of Si and Al with a quaternary template.[28] Dealumination, which is evident from ^{27}Al MAS NMR (Fig. 7), results in an increase in the concentration of Lewis sites at the expense of Brønsted sites.

(b) By post-synthesis. The generation of acid sites by post-treatment of siliceous mesoporous materials with aluminium salts is widely reported.[16,17–22,28] Typically, grafting of aluminium has involved liquid–solid reactions using aluminium as the isopropoxide,[16,21,28] chlorohydrate,[18,22] nitrate,[20] chloride,[9] *etc.* In the case of $AlCl_3$ and $Al(OPr^i)_3$ a non-aqueous liquid phase is often used, for example ethanol, hexane or chloroform, and wet impregnation of siliceous mesoporous materials with $Al(NO_3)_3$ also results in increased concentrations of Brønsted and Lewis sites.[16,20] However, the concentration of acid sites, determined from pyridine sorption, is reported[21] for the alumination of siliceous MCM-41 using a solution of $AlCl_3$ in chloroform and a solution of aluminium isopropoxide. These results are compared with results reported here for the corresponding gas/solid phase reaction [Fig. 9(b)].

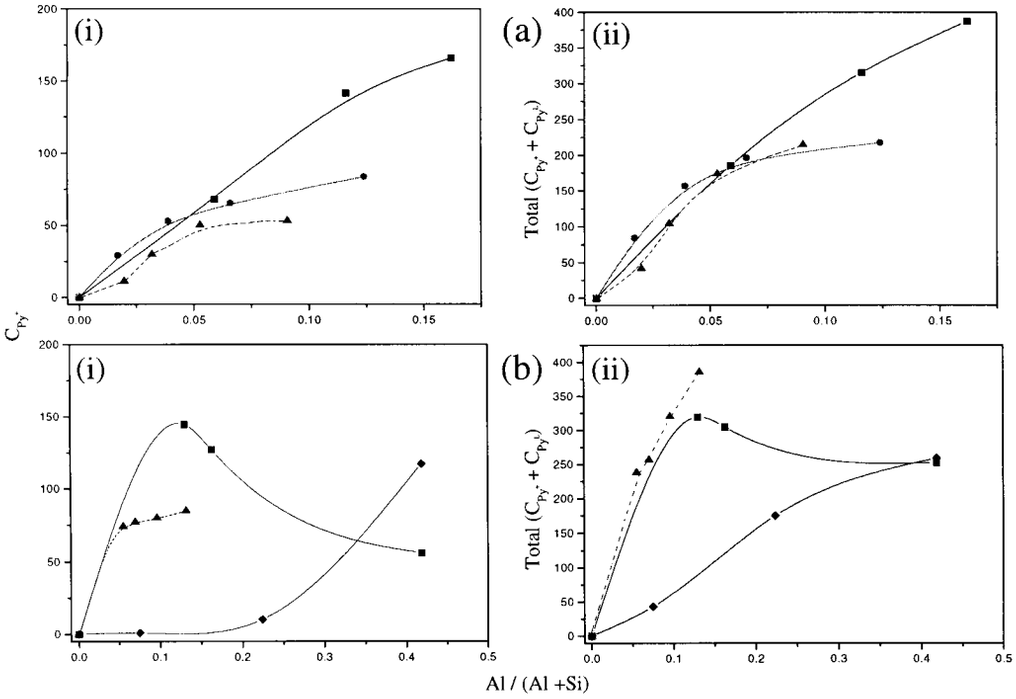

Fig. 9 Relationship between the concentration of Brønsted sites and total acid sites (Brønsted + Lewis) on the aluminium fraction of AlMCM-41: (a) direct synthesis and (b) post-synthesis. (■) Chen *et al.*,[21] (●) Mokaya and Jones,[22] (■) Chen *et al.*[21] and (▲) present study.

The present results for the gas/solid reaction between $AlCl_3$ and siliceous MCM-41 lead to an increase in both Brønsted and Lewis acidity for the post-synthesis when compared with directly synthesised materials with a similar aluminium fraction. The reaction of siliceous MCM-41 with $AlCl_3$ vapour results, initially, in a relatively large increase in the concentration of Brønsted sites [Fig. 9(b)]. Treatment with increasing amounts of $AlCl_3$ produces a much smaller increase in Brønsted site concentration with increase in aluminium fraction as discussed above and implied by Fig. 9(b-i). Moreover, for this region the ratio of Lewis/Brønsted sites increases linearly with aluminium fraction. These results can be explained if we assume that there is a limit to the surface sites, on a given sample of SiMCM-41, which are suitable for facile generation of bridged hydroxyl [≡Al(OH)Si≡] by reaction with $AlCl_3$ vapour [eqn. (2)]. Consequently, after these surface sites are consumed, by reaction with $AlCl_3$, additional $AlCl_3$ would, for the most part, be deposited and, after hydrolysis, result in increasing amounts of extraframework aluminium with an associated increase in Lewis sites. A similar explanation has been reported for the aqueous phase reaction of aluminium chlorohydrate with siliceous MCM-41.[22] However, the above pattern, for treatment with $AlCl_3$ vapour, differs from the study of Chen *et al.*[21] who used $AlCl_3$ in hexane solution and observed an initial increase in acid site concentration, as above, followed by a decrease as the aluminium fraction increased [Fig. 9(b)]. More interestingly, post-treatment of SiMCM-41 with a solution of aluminium isopropoxide did not show any initial increase in Brønsted site concentration, and the dependence on aluminium fraction was completely different from that obtained by reaction with a solution of aluminium chloride [Fig. 9(b)].

(c) Comparison of catalytic activity on directly and post-synthesised materials. Although catalytic and ^{27}Al MAS NMR results are frequently quoted, acid site concentration determined by the FTIR analysis of sorbed pyridine is not generally available from previous studies. However, several papers report both acid site concentrations and catalytic results for the conversion of cumene over mesoporous acid catalysts.[21,22,28] In the present study catalytic activity was assessed by the conversion of 1,3,5-TIPB which has been less widely studied. The present catalytic runs were made using the same flow rates and weight of catalyst in each case and are recorded as relative first order rate constants $\ln[1/(1-x)]$ where x is the fractional conversion. A separate study[30] demonstrated that the overall conversion of 1,3,5-TIPB could be represented by a first order process. Fig. 10 shows catalytic results for the present study and for the conversion of cumene reported by both Chen *et al.*[21] and Mokaya *et al.*[22,28] Assuming first order conversion of cumene, a relative first order rate constant is used for the correlation of the results by Chen *et al.*[21] and the reported initial reaction rates are used to correlate the results of Mokaya *et al.*[22]

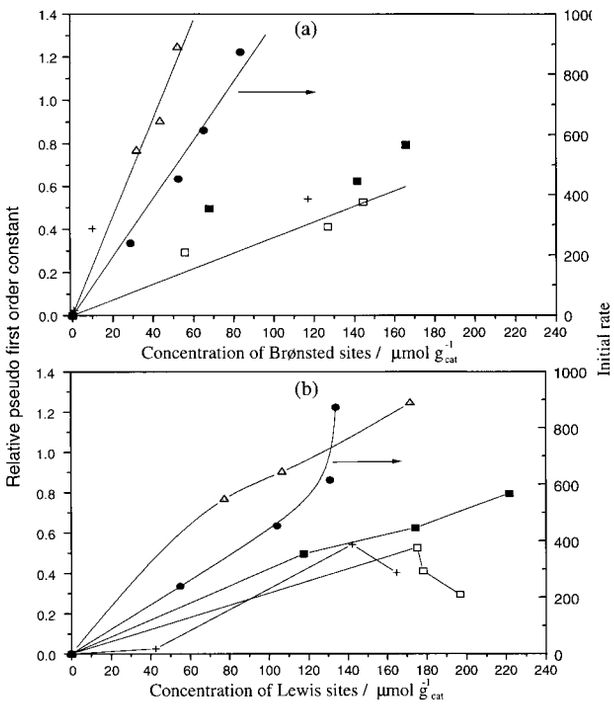

Fig. 10 Dependence of catalytic activity in the conversion of 1,3,5-TIPB (present study) and cumene[21,22] on acid site concentration (a) Brønsted sites and (b) Lewis sites. Catalysts prepared by direct synthesis (▲) present study, (●) Mokaya *et al.*[22] and (■) Chen *et al.*[21] Catalysts prepared by post-synthesis (□) and (+) Chen *et al.*[21]

In general, for the AlMCM-41 materials synthesised directly by Mokaya *et al.*[13] and in the present study, the correlation of initial rate (or relative rate constant) at 300 °C shows a better correlation with the concentration of Brønsted sites [Fig. 10(a)] than with the concentration of Lewis sites [Fig. 10(b)], in keeping with the view that conversion of cumene and, presumably, 1,3,5-TIPB are catalysed by Brønsted acid sites. However, in view of the limited amount of data and because of the approximate correlation between Brønsted and Lewis site concentration, for the directly synthesised materials, it is not possible to exclude completely a catalytic role for Lewis sites, on the basis of the results shown in Fig. 10.

Similar results are observed for cumene conversion over the directly synthesised materials of Chen *et al.*,[21] and, although there appears to be more scatter, the number of points is too few to make meaningful statistical analysis [Fig. 10(a)]. Moreover, the effects of any deactivation cannot be taken into account in the work reported by Chen *et al.*[21] What is clear from the study of Chen *et al.*[21] is that there is no evidence for an increase in reaction rate with increase in Lewis site concentration [Fig. 10(b)], supporting a role for Brønsted rather than Lewis sites in the conversion of cumene. Of course, any sites of enhanced Brønsted acidity produced by Lewis–Brønsted interaction could also be involved.[36,39]

Conclusion

In the present study it was demonstrated that aluminium can be successfully incorporated into purely siliceous mesoporous MCM-41 (SiMCM-41) by a post-synthesis reaction with aluminium chloride vapour. Materials prepared by this post synthesis reaction were compared with a series of AlMCM-41 catalysts where aluminium was incorporated during synthesis. The MAS NMR spectroscopic findings clearly show that both methods yield materials where aluminium is located at both framework and extraframework sites. It is also evident that a considerable amount of aluminium moves to extraframework sites during calcination of the ammonium form to produce the hydrogen form of the directly synthesised catalysts.

Over a similar range of aluminium fraction, in the solids, the concentrations of both Brønsted and Lewis acid sites (accessible to pyridine) were higher for the post-synthesised materials. This was reflected in the catalytic activity (conversion of 1,3,5-TIPB) which was also higher for the post-synthesised catalysts.

Comparison of the present results with previously published data shows a wide range in the concentration of acid sites, corresponding to given levels of aluminium in the solids, depending upon method of incorporation. Syntheses based on alkoxides of silicon and aluminium can, in general, generate higher concentrations of acid sites, particularly at higher levels of aluminium incorporation, than syntheses based on typical inorganic sources of Si and Al. However, especially at higher

levels of aluminium, there appears to be considerable variation in acid site concentrations even when similar synthesis compositions are used. Comparison of the present catalytic results for conversion of 1,3,5-TIPB with results reported for cumene conversion shows a better correlation between catalytic activity and Brønsted acid site concentration than with Lewis acid site concentration, in agreement with the view that this is a predominantly Brønsted acid catalysed reaction.

Acknowledgements

The authors wish to thank the Danish Government, EPSRC and BNFL, Engelhart and ICI for financial support.

References

1 D. H. Olson, W. O. Haag and R. M. Lago, *J. Catal.*, 1980, **61**, 390.
2 J. Dwyer, *NATO ASI Ser., Ser. C*, 1991, **352**, 303.
3 R. M. Dessau and G. T. Kerr, *Zeolites*, 1984, **4**, 315.
4 C. D. Chang, C. T.-W. Chu, J. N. Miale, R. F. Bridger and R. B. Calvert, *J. Am. Chem. Soc.*, 1984, **106**, 8143.
5 Z. Zhang, X. Liu, Y. Xu and R. Xu, *Zeolites*, 1991, **11**, 232.
6 X. Liu, J. Klinowski and J. Thomas, *J. Chem. Soc., Chem. Commun.*, 1986, 582.
7 M. Janicke, D. Kumar, G. D. Stucky and B. F. Chmelka, *Stud. Surf. Sci. Catal.*, 1994, **84**, 243.
8 Z. Luan, C.-F. Chang, W. Zhou and J. Klinowski, *J. Phys. Chem.*, 1995, **99**, 1018.
9 S. Sato and G. E. Maciel, *J. Mol. Catal. A: Chem.*, 1995, **101**, 153.
10 M. Busio, J. Jänchen and J. H. C. van Hooff, *Microporous Mater.*, 1995, **5**, 211.
11 R. B. Borade and A. Clearfield, *Catal. Lett.*, 1995, **31**, 267.
12 K. R. Kloetstra, H. W. Zandbergen and H. van Bekkum, *Catal. Lett.*, 1995, **33**, 157.
13 R. Mokaya, W. Jones, Z. Luan, M. D. Alba and J. Klinowski, *Catal. Lett.*, 1996, **37**, 113.
14 A. Liepold, K. Roos, W. Reschetilowski, A. P. Esculcas, J. Rocha, A. Philippou and M. W. Anderson, *J. Chem. Soc., Faraday Trans.*, 1996, **92**, 4623.
15 H. Hamdan, S. Endud, H. He, M. N. M. Muhid and J. Klinowski, *J. Chem. Soc., Faraday Trans.*, 1996, **92**, 2311.
16 R. Mokaya and W. Jones, *Chem. Commun.*, 1997, 2185.
17 M. Chatterjee, T. Iwasaki, H. Hayashi, Y. Onodera, T. Ebina and T. Nagase, *Catal. Lett.*, 1998, **52**, 21.
18 R. Mokaya and W. Jones, *Chem. Commun.*, 1998, 1839.
19 R. Anwander, C. Palm, O. Groeger and G. Engelhardt, *Organometallics*, 1998, **17**, 2027.
20 S.-C. Shen and S. Kawi, *Chem. Lett.*, 1999, 1293.
21 L. Y. Chen, Z. Ping, G. K. Chuah, S. Jaenicke and G. Simon, *Micropor. Mesopor. Mater.*, 1999, **27**, 231.
22 R. Mokaya and W. Jones, *J. Mater. Chem.*, 1999, **9**, 555.
23 J. S. Beck, J. C. Vartuli, W. J. Roth, M. E. Leonowicz, C. T. Kresge, K. D. Schmitt, C. T.-W. Chu, D. H. Olson, E. W. Sheppard, S. B. McCullen, J. B. Higgins and J. L. Schlenker, *J. Am. Chem. Soc.*, 1992, **114**, 10834.
24 A. Corma, V. Fornes, M. T. Navarro and J. Perez-Pariente, *J. Catal.*, 1994, **148**, 569.
25 F. Di Renzo, B. Chiche, F. Fajula, S. Viale and E. Garrone, *Stud. Surf. Sci. Catal.*, 1996, **101**, 851.
26 J. Weglarski, J. Datka, H. He and J. Klinowski, *J. Chem. Soc., Faraday Trans.*, 1996, **92**, 5161.
27 H. Kosslick, H. Landmesser and R. Fricke, *J. Chem. Soc., Faraday Trans.*, 1997, **93**, 1849.
28 R. Mokaya and W. Jones, *J. Catal.*, 1997, **172**, 211.
29 R. M. Dessau and G. T. Kerr,US Patent no. 4438215, 1984.
30 A. Ghanbari-Siahkali, Ph.D. Thesis, University of Manchester, Institute of Science and Technology, Manchester, 1999.
31 P. J. Branton, P. G. Hall and K. S. W. Sing, *J. Chem. Soc., Chem. Commun.*, 1993, 1257.
32 C. A. Emeis, *J. Catal.*, 1993, **141**, 347.
33 M. A. Makarova, K. Khalid and J. Dwyer, *J. Micropor. Mater.*, 1995, **4**, 243.
34 J. W. Ward, *Zeolite Chemistry and Catalysis*, ACS Monograph 171, ed. J. A. Rabo, ACS, Washington DC, 1976.
35 A. Ghanbari-Siahkali, A. Philippou, J. Dwyer and M. W. Anderson, *Appl. Catal. A*, 2000, **192**, 57.
36 J. Dwyer, V. Zholobenko, A. Khodakov, S. Bates and M. A. Makarova, *Stud. Surf. Sci. Catal.*, 1996, **105**, 181.
37 T. R. Hughes and H. M. White, *J. Phys. Chem.*, 1967, **71**, 2192.
38 L. Mariey, S. Khabtou, J. C. Lavalley, A. Chambellan and T. Chevreau, *Stud. Surf. Sci. Catal.*, 1995, **97**, 501.
39 M. Makarova, S. P. Bates and J. Dwyer, *J. Am. Chem. Soc.*, 1995, **117**, 11308.